CARBON 47 (2009) 731–736

available at www.sciencedirect.com

ScienceDirect

journal homepage: www.elsevier.com/locate/carbon

Semiconducting properties of cup-stacked carbon nanotubes

*Qingfeng Liu, Wencai Ren, Zhi-Gang Chen, Lichang Yin, Feng Li, Hongtao Cong, Hui-Ming Cheng**

Shenyang National Laboratory for Materials Science, Institute of Metal Research, Chinese Academy of Sciences, Shenyang 110016, China

ARTICLE INFO

Article history:
Received 3 September 2008
Accepted 5 November 2008
Available online 13 November 2008

ABSTRACT

The current–voltage characteristics of individual cup-stacked carbon nanotubes (CSCNTs) were investigated in situ inside the transmission electron microscope. Different from other quasi-1D carbon structures such as multi-walled carbon nanotubes, carbon nanofibers or graphitic fibers that normally behave as a metallic conductor of electrons, individual CSCNTs were found to exhibit unexpectedly semiconducting behaviors due to the special stacking microstructure of graphene layers. The band gap of the CSCNTs was obtained with the value of about 0.44 eV, in contrast to the zero-gap semiconducting quasi-2D graphene. These findings provide new information about the effect of the stacking graphene layers on their electronic properties, and will widen the usefulness of such stacking structure for the application in nanoelectronics.

1. Introduction

Numerous applications of carbon nanotubes (CNTs), e.g. field-effect transistors [1], light-emitting diodes [2] and molecular electronic devices [3], require an understanding of their electronic properties. The electronic transport properties of single-walled carbon nanotubes (SWCNTs) are either metallic or semiconducting, dependent on their diameter and chirality denoted by the structural indices (n, m) [4]. For instance, about one-third of SWCNTs exhibit metallic properties (if $n-m = 3p$, where p is an integer) while the remaining two-thirds act as semiconductor ($n-m = 3p \pm 1$) [5]. However, other quasi-1D carbon structures such as multi-walled carbon nanotubes (MWCNTs) [6], carbon nanofibers (CNFs) [7] or graphitic fibers normally behave as a metallic conductor of electrons with properties similar to perfect graphite along graphene layers [8]. Interestingly, perfect graphite exhibits conducting behaviors along to graphene layer, but insulating behaviors perpendicular to graphene layer, because of the different effective mass of carriers in different lattice directions [8].

Recently, cup-stacked carbon nanotubes (CSCNTs) [9,10] have attracted increasing attention as a special and functional nanosized material in heterogeneous catalysis, solar cells, etc. From the morphological viewpoint, CSCNTs consist of many truncated conical graphene layers, different from conventional CNTs made up of multi-seamless cylinders of hexagonal carbon networks [11]. Such a structure provides a large portion of exposed and reactive edges with abundant dangling bonds both on the outer surface and in the inner channel. In addition, the chemical activity of the inner channel is even higher due to highly strained curvature [12]. So the utilization of these exposed edges of CSCNTs to chemical functionalization or surface modification opens up new avenues in absorbent materials, composites, field emitters, gas storage components, and heterogeneous catalysis [13–15]. However, an important question that still remains to be addressed is about the electronic property of CSCNTs.

* *Corresponding author:* Fax: +86 24 2390 3126.
E-mail address: cheng@imr.ac.cn (H.-M. Cheng).
0008-6223/$ - see front matter
doi:10.1016/j.carbon.2008.11.005

In this work, we measured the electrical transport behaviors of individual CSCNTs inside a transmission electron microscope (TEM) using a piezo-driven scanning tunneling microscopy (STM) holder. It was found that individual CSCNTs exhibited unexpected semiconducting current–voltage characteristics, different from conventional quasi-1D carbon structures such as MWCNTs and CNFs. These findings will widen the usefulness of such stacking structure for the application in nanoelectronics in the fields of semiconductor.

2. Experimental

Metallocenes such as ferrocene have been demonstrated to be used as precursors to prepare carbon nanostructures, because they can not only act as carbon source but also give rise to small metal clusters as catalyst [16–18]. Here high-quality CSCNTs with short lengths (<3.5 μm) was grown in a quartz tube reactor inside a dual-zone furnace. Generally, a quantity of ferrocene with sulfur (S = 2–5 wt%) as growth promoter was fast sublimated in the first zone at ~300 °C, and transported into the second zone by Ar flow of ~2000 sccm (standard cubic centimeter per minute), where pyrolysis occurred at elevated temperatures of ~1100 °C. After a growth time of ~5 min, the furnace was cooled naturally to room temperature under the protection of Ar. The selected clean CSCNTs without iron particles were glued to a gold wire (about 0.25 mm in diameter and about 4.0 mm in length) connected to an electrode inside a TEM. The free end of a single CSCNT was approached and contacted with an etched tungsten (W) tip connected to another electrode, thus completing a circuit between the tungsten tip and the sample that can be held at an arbitrary voltage (a maximum voltage ±140 V). Such setup was integrated into a TEM sample holder, which enables concurrently microstructure observation and *I–V* measurements [19–25].

3. Results and discussion

Fig. 1a is a typical TEM image of the as-grown CSCNTs. These CSCNTs have a large hollow core along their length and an iron particle encapsulated in their tips. Ratios of the inner diameter (60–100 nm) over the outer diameter (80–120 nm) of the CSCNTs mainly range from 0.61 to 0.75. Fig. 1b is a high-resolution TEM (HRTEM) image of the CSCNT wall. The lattice fringe spacing on the CSCNT wall is about 0.335 nm, close to that of the graphite (002) plane. Such observations are attributed to a superposition of the conical graphene cups, which in turn provides a large portion of exposed edges on the outer surface and in the inner channel of the hollow nanotube. The truncated cone angle (cup) with regard to the tube axis is found to lie mainly in a narrow range of 10–30°, and no nanotubes are found to have a cone angle larger than 50°. Apparently, it is difficult to close the two adjacent graphitic layers by eliminating the dangling bonds for the nanotube with a small cone angle, because of the large distance between the dangling bonds located at the edges of two adjacent layers. The clear wall of the CSCNT demonstrates the stacking structure of truncated conical graphene layers, as schematically shown in the inset in Fig. 1b. Moreover, the outer surface of the CSCNT is very clean and scarcely covered by amorphous carbon, when compared to previously-synthesized CSCNTs [9].

Fig. 2a shows a CSCNT of about 600 nm in length connected to two metal electrodes inside the TEM. To make a good electrical contact, i.e. ohmic contact, between the CSCNT and metal electrodes, several tens of voltage sweeps of 0–2 V (to avoid the breakdown of the CSCNT) was first applied to pass through this electrode-nanotube-electrode circuit, as shown in Fig. 2b. High resistance of the contact point induced to generate high temperature, which welded the metal electrodes to the CSCNT and generated a perfect contact between them. The typical *I–V* curves obtained for the CSCNT after 690 and 726 sweeps (before its breakdown) are shown in Fig. 2c. It can be seen that after the formation of good contacts between the electrodes and the nanotube, the *I–V* curves of the nanotube keep similar before the nanotube break down. In general, the *I–V* characteristics basically demonstrate a semiconducting CSCNT. It should be noted that during the 727th sweep, the nanotube broke down, which may be initiated by resistive heating at the heat-stimulated imperfections (i.e., some localized positions with defects) [21].

Clearly, the measured system as a whole can be regarded as a metal-semiconductor-metal (M-S-M) series circuit, which is composed of two Schottky barriers formed at the two con-

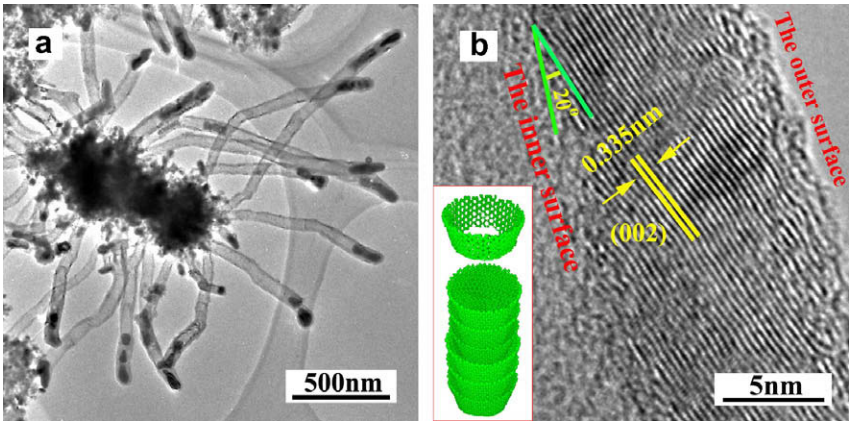

Fig. 1 – (a) TEM image of the as-synthesized CSCNTs with short lengths. (b) HRTEM image of the CSCNT wall. The inset in (b) is a schematic of a CSCNT.

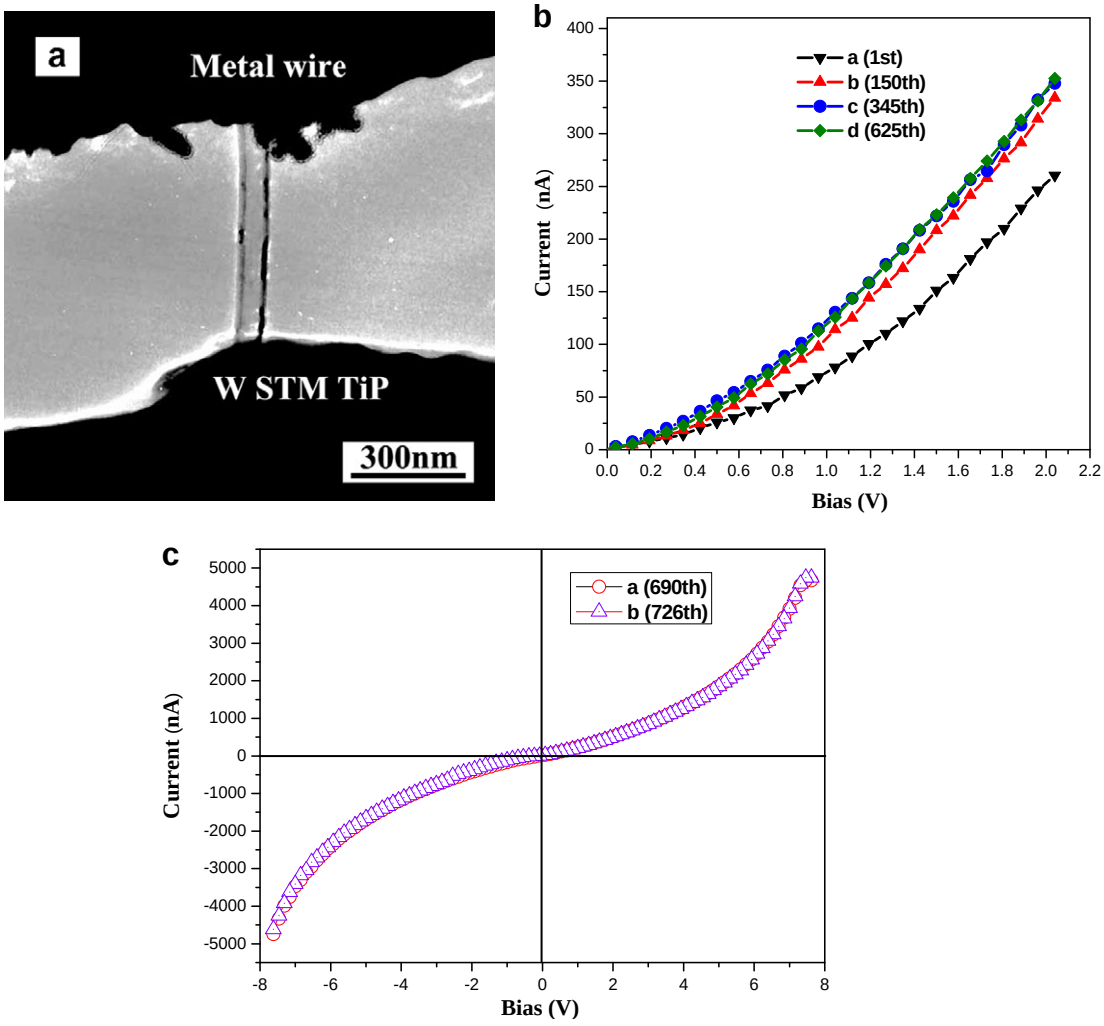

Fig. 2 – (a) TEM image of a typical CSCNT connected to two metal electrodes. (b) *I–V* curves for different voltage sweeps in order to make a good electrical contact between the CSCNT and metal electrodes. (c) Typical *I–V* curves of the same CSCNT in (a) after 690 and 726 voltage sweeps before its breakdown.

tacts and one resistor (i.e. the CSCNT) in between. Therefore, the total voltage is equivalent to the sum of each sub voltage for each element, as expressed by the following equation:

$$V = V_1 + V_{NT} + V_2 \quad (1)$$

where V_1, V_{NT}, and V_2 are voltages on Schottky barrier I (tip-CSCNT), the CSCNT, and Schottky barrier II (CSCNT-wire), respectively. And the current flowing through such series circuit is the same for each element with

$$I = S_1 J_1 + V_1/R_{sh1} = V_{NT}/R = S_2 J_2 + V_2/R_{sh2} \quad (2)$$

where R is the resistance of the CSCNT, S_1 and S_2 are the contact areas of Schottky barrier 1 and 2, respectively, J_1 and J_2 are the current density through the Schottky barrier 1 and 2, respectively, and R_{sh1} and R_{sh2} are the shunt resistance of barrier 1 and 2, respectively. It is worthy noting that such shunt resistances have noticeable effects on the transport property of a Schottky contact at low bias [26]. From Fig. 2c, it can be seen that the current passing through the circuit is very small at very low bias, because the total voltage is distributed mainly on the two Schottky barriers, i.e. $V_1, V_2 \gg V_{NT}$.

At high bias (i.e. $V > 2.0$ V), the thickness reduction of a Schottky barrier for electron tunneling becomes less effective [26], and thus the relative voltage drop decreases rapidly. Meanwhile, the voltage drop of the CSCNT increases continuously and finally approaches the value of total voltage of the circuit, suggesting that the resistance of the nanotube is equivalent to the total differential resistance of the circuit, and that the voltage on the nanotube increases almost linearly with the bias and becomes the dominating term when the current is notable. Therefore, each applied voltage V corresponds to a unique current I.

Numerically we can differentiate the *I–V* curve to obtain the resistance (Fig. 3a) of the CSCNT directly in the large current regime, i.e.

$$R = \frac{dV_{NT}}{dI} = a_{NT}\frac{dV}{dI} \approx \frac{dV}{dI} \quad (3)$$

where the voltage drop factor a_{NT} is defined to describe relative voltage drop of the nanotube on the three components of the circuit, i.e. $a_{NT} = dV_{NT}/dV$. By the way, Zhang et al. [23] believed that for reverse bias voltage V and intermediate

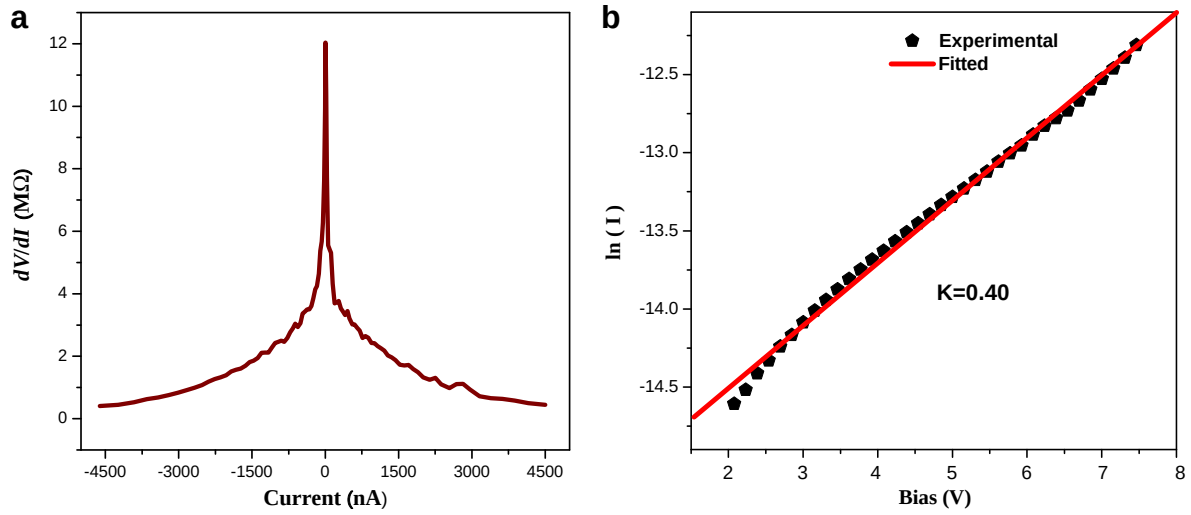

Fig. 3 – (a) Corresponding dV/dI curve of the CSCNT and (b) experimental and fitted plot of ln *I* vs. *V* from the *I*–*V* curve after 726 voltage sweeps in Fig. 2c.

temperature, the tunneling current is mainly the thermionic-field emission current. Neglecting the leaking current that is notable only at very low bias, the dependence of the total current on the total voltage can be given by the following equation[23,24,26,27]:

$$\ln I = \ln(SJ) = \ln S + V\left(\frac{q}{kT} - \frac{1}{E_0}\right) + \ln J_s \quad (4)$$

where J is the current density through the Schottky barrier, S is the contact area associated with a barrier, E_0 is a parameter that depends on the carrier density, and J_s is a slowly varying function of an applied bias. Depending on the Eq. (4), we can obtain the semiconductor parameters from the *I*–*V* curves in the intermediate bias regime where the reverse-biased Schottky barrier dominates the total current [24]. For example, a logarithmic plot of the current I as a function of the bias V follows approximately a linear relationship, as shown in Fig. 3b. In addition, the slop ($q/kT - 1/E_0$) of the straight line is independent of the contacts and only determined by the electrical properties of the semiconductor. Here, we can obtain E_0 = 26.15 mV. Meanwhile, E_0 can also be given by the following equation[23,24,27]:

$$E_0 = E_{00}\coth\left(\frac{qE_{00}}{kT}\right) = \frac{\hbar}{2}\left[\frac{N_d}{m_n^*\varepsilon_s\varepsilon_0}\right]^{\frac{1}{2}}\coth\left(\frac{qE_{00}}{kT}\right) \quad (5)$$

where N_d, m_n^*, ε_s and ε_0 are the donor density at the metal/semiconductor interface, the effective mass of electron, relative permittivity of the semiconducting CSCNT, the permittivity of free space, respectively. In tunneling theory, the parameter of E_{00} reflects the diffusion potential of a Schottky barrier, i.e. the transmission probability for an electron whose energy coincides with the bottom of the conduction band at the edge of the depletion region [26]. From Eq. (5), we can obtain the electron concentration at the metal/semiconductor interface, i.e. $N_d = 1.13\times10^{17}$ cm^{-3}, about 10^{-4} electrons per atom, well in agreement with that of usual graphitic material.

It is known that for an intrinsic semiconductor the concentration of carriers n_i can be give by the following equation[23]:

$$n_i = \left[\frac{2(2\pi kt)^{3/2}(m_h^* m_n^*)^{3/4}}{h^3}\right]\exp\left(-\frac{E_g}{2kT}\right) \quad (6)$$

where m_h^* and E_g are the effective mass of hole and the bandgap of the semiconducting CSCNT, respectively. Therefore we can obtain the bandgap of the CSCNT, i.e. $E_g \approx 0.44$ eV, in contrast to the zero-gap semiconducting quasi-2D graphene [28].

We carried out many analogous experiments by changing CSCNTs with different diameters and lengths to investigate the current–voltage characteristics of the CSCNTs. The similar electronic transition was observed. The resistance of the CSCNTs ranges from 0.3 MΩ to 20 MΩ, a factor of 10^3 higher than these of conventional MWCNTs with similar diameter and length. Such semiconducting property of CSCNTs will greatly enlarge the applications of such quasi-1D carbon nanostructures in many fields. For example, conventional CNTs have not been fully explored for use in photovoltaic applications due to their poor charge separation efficiency, while CSCNT-based solar cells exhibit a superior performance, even comparable to that of photo electrochemical cells based on some nanostructured semiconductors of TiO_2, ZnO, CdS, etc [29].

The semiconducting electronic properties of the CSCNTs are attributed to their unique stacking microstructure of graphene layers (cups). It is known that highly oriented pyrolytic graphite (HOPG) with typical quasi-2D layered structure is a paradigm of anisotropic systems in nature [8]. For example, conducting and insulating electrical transport behaviors are in the coexistence of HOPG along and perpendicular to graphene layers, respectively, which has its origin in the different effective mass of carriers in different lattice directions [8]. Conventional MWCNTs made up of many seamless cylinders of hexagonal carbon networks have an electrical conductivity that is along the graphene layers, and therefore are basically metallic [21]. In stark contrast, the CSCNTs have a stacking structure of truncated conical graphene layers so that their electronic transport across planes rather than along planes should be much less conducting than that of MWCNTs. It is worthy noting that the closing of the graphene

layer into a cup shape may be one of the most important reasons for the energy gap of CSCNTs, and further studies are required to elucidate this point. On the other hand, the defects distributing on the outer/inner surface of CSCNT walls may have an important influence on their electronic properties. A large portion of exposed and reactive edges with highly strained curvature imply the existence of a higher defect density such as pentagons, heptagons, dangling bonds, or any others both on the outer surface and in the inner channel of CSCNTs. These defects may change the density of states [8], make the graphene cups a better linkage and coupling in the quasi *c*-axis direction, and thus provide the conducting regions that percolate. This will provide an excess of charge on these open curved edges, changing the CSCNTs from insulating into semiconducting electrical transport properties.

4. Conclusions

When compared to conventional MWCNTs and CNFs with metallic electrical transport properties, individual CSCNTs exhibit a striking semiconducting electronic transport, resulting from their special stacking microstructure of graphene layers. The band gap of the CSCNTs was obtained with the value of about 0.44 eV, in contrast to the zero-gap semiconducting quasi-2D graphene. These findings provide new information about the effect of the stacking graphene layers on their electronic properties, and will widen the usefulness of such stacking structure for the application in nanoelectronics.

Acknowledgements

The work was supported by Ministry of Science and Technology of China (No. 2006CB932703 and No. 2008DFA51400), National Science Foundation of China (No. 90606008 and No. 50702063), and Chinese Academy of Sciences (No. KJCX2-YW-M01).

REFERENCES

[1] Unalan HE, Fanchini G, Kanwal A, Du Pasquier A, Chhowalla M. Design criteria for transparent single-wall carbon nanotube thin-film transistors. Nano Lett 2006;6(4):677–82.
[2] Zhang DH, Ryu K, Liu XL, Polikarpov E, Ly J, Tompson ME, et al. Transparent, conductive, and flexible carbon nanotube films and their application in organic light-emitting diodes. Nano Lett 2006;6(9):1880–6.
[3] Liu QF, Ren WC, Li F, Cong HT, Cheng HM. Synthesis and high thermal stability of double-walled carbon nanotubes using nickel formate dihydrate as catalyst precursor. J Phys Chem C 2007;111(13):5006–13.
[4] Liu QF, Ren WC, Chen ZG, Wang DW, Liu BL, Yu B, et al. Diameter-selective growth of single-walled carbon nanotubes with high quality by floating catalyst method. ACS Nano 2008;2(8):1722–8.
[5] Dresselhaus MS. Nanotubes – a step in synthesis. Nat Mater 2004;3(10):665–6.
[6] Wang MS, Wang JY, Chen Q, Peng LM. Fabrication and electrical and mechanical properties of carbon nanotube interconnections. Adv Funct Mater 2005;15(11):1825–31.
[7] Yang XJ, Guillorn MA, Austin D, Melechko AV, Cui HT, Meyer HM, et al. Fabrication and characterization of carbon nanofiber-based vertically integrated Schottky barrier junction diodes. Nano Lett 2003;3(12):1751–5.
[8] Lu YH, Munoz M, Steplecaru CS, Hao C, Bai M, Garcia N, et al. Electrostatic force microscopy on oriented graphite surfaces: coexistence of insulating and conducting behaviors. Phys Rev Lett 2006;97(7):076805-1–4.
[9] Endo M, Kim YA, Hayashi T, Fukai Y, Oshida K, Terrones M, et al. Structural characterization of cup-stacked-type nanofibers with an entirely hollow core. Appl Phys Lett 2002;80(7):1267–9.
[10] Kim YA, Hayashi T, Fukai Y, Endo M, Yanagisawa T, Dresselhaus MS. Effect of ball milling on morphology of cup-stacked carbon nanotubes. Chem Phys Lett 2002;355(3–4):279–84.
[11] Saito K, Ohtani M, Fukuzumi S. Electron-transfer reduction of cup-stacked carbon nanotubes affording cup-shaped carbons with controlled diameter and size. J Am Chem Soc 2006;128(44):14216–7.
[12] Endo M, Kim YA, Ezaka M, Osada K, Yanagisawa T, Hayashi T, et al. Selective and efficient impregnation of metal nanoparticles on cup-stacked-type carbon nanofibers. Nano Lett 2003;3(6):723–6.
[13] Kim C, Kim YJ, Kim YA, Yanagisawa T, Park KC, Endo M, et al. High performance of cup-stacked-type carbon nanotubes as a Pt–Ru catalyst support for fuel cell applications. J Appl Phys 2004;96(10):5903–5.
[14] Choi YK, Gotoh Y, Sugimoto KI, Song SM, Yanagisawa T, Endo M. Processing and characterization of epoxy nanocomposites reinforced by cup-stacked carbon nanotubes. Polymer 2005;46(25):11489–98.
[15] Shiratori Y, Hiraoka H, Takeuchi Y, Itoh S, Yamamoto M. One-step formation of aligned carbon nanotube field emitters at 400 degrees C. Appl Phys Lett 2003;82(15):2485–7.
[16] Cheng HM, Li F, Su G, Pan HY, He LL, Sun X, et al. Large-scale and low-cost synthesis of single-walled carbon nanotubes by the catalytic pyrolysis of hydrocarbons. Appl Phys Lett 1998;72(25):3282–4.
[17] Liu QF, Ren WC, Chen ZG, Liu BL, Yu B, Li F, et al. Direct synthesis of carbon nanotubes decorated with size-controllable Fe nanoparticles encapsulated by graphitic layers. Carbon 2008;46(11):1417–23.
[18] Liu QF, Chen ZG, Liu BL, Ren WC, Li F, Cong HT, et al. Synthesis of different magnetic carbon nanostructures by the pyrolysis of ferrocene at different sublimation temperatures. Carbon 2008;46(14):1892–902.
[19] Svensson K, Olin H, Olsson E. Nanopipettes for metal transport. Phys Rev Lett 2004;93(14):145901-1–4.
[20] Chen S, Huang JY, Wang Z, Kempa K, Chen G, Ren ZF. High-bias-induced structure and the corresponding electronic property changes in carbon nanotubes. Appl Phys Lett 2005;87(26):263107-1–3.
[21] Huang JY, Chen S, Jo SH, Wang Z, Han DX, Chen G, et al. Atomic-scale imaging of wall-by-wall breakdown and concurrent transport measurements in multiwall carbon nanotubes. Phys Rev Lett 2005;94(23):236802-1–4.
[22] Huang JY, Kempa K, Jo SH, Chen S, Ren ZF. Giant field enhancement at carbon nanotube tips induced by multistage effect. Appl Phys Lett 2005;87(5):053110-1–3.
[23] Zhang ZY, Jin CH, Liang XL, Chen Q, Peng LM. Current–voltage characteristics and parameter retrieval of semiconducting nanowires. Appl Phys Lett 2006;88(7):073102-1–3.
[24] Bai XD, Golberg D, Bando Y, Zhi CY, Tang CC, Mitome M, et al. Deformation-driven electrical transport of individual boron nitride nanotubes. Nano Lett 2007;7(3):632–7.
[25] Huang JY, Chen S, Ren ZF, Wang Z, Kempa K, Naughton MJ, et al. Enhanced ductile behavior of tensile-elongated

individual double-walled and triple-walled carbon nanotubes at high temperatures. Phys Rev Lett 2007;98(18):185501-1–4.
[26] Zhang ZY, Yao K, Liu Y, Jin CH, Liang XL, Chen Q, et al. Quantitative analysis of current–voltage characteristics of semiconducting nanowires: decoupling of contact effects. Adv Funct Mater 2007;17(14):2478–89.
[27] Padovani FA, Stratton R. Field and thermionic-field emission in Schottky barriers. Solid-State Electronics 1966;9(7):695–707.
[28] Geim AK, Novoselov KS. The rise of graphene. Nat Mater 2007;6(3):183–91.
[29] Hasobe T, Fukuzumi S, Kamat PV. Stacked-cup carbon nanotubes for photoelectrochemical solar cells. Angew Chem-Int Edit 2006;45(5):755–9.